Quest Journals
Journal of Research in Environmental and Earth Sciences
Volume 8 ~ Issue 5 (2022) pp: 42-50
ISSN(Online) :2348-2532
www.questjournals.org

Research Paper

Map Based Gravity and Magnetic Interpretation: The Officer Basin as case Study

Onengiyeofori A. Davies[1] and Prince N. Nwiyor[2]
[1]*Physics Department, Rivers State University, Port Harcourt, Rivers State, Nigeria*
[2] *Science Laboratory Technology Department, Ken Saro Wiwa Polytechnic, Bori, Nigeria*
Corresponding Author: Onengiyeofori A. Davies

ABSTRACT: *A regional scale interpretation was carried out on the Officer Basin, which has been previously poorly explored, using gravity and magnetic data which are subsets of the regional grid of the whole Australia. The Edges of the Basin was delineated from the analytical signal of the reduced to pole grid of the total magnetic intensity within which five Sub-Basins were identified. The Basin is generally trending from NW to SE with the deepest part, at an estimated depth of 9.8km, at the NW end within the delineated Sub-Basin at that end. Key features interpreted within the Officer Basin include a huge thrust fault at the Northern edge of the Basins, Series of pluton running symmetrically along a plane NS in the middle of the basin, ridges and dykes. Due to the poorly explored nature of the Officer Basin, there was little information available to aid in constraining the interpretation presented in this report, especially the quantitative interpretation.*
KEYWORDS: *Gravity, Magnetic, Mapping, Lineament Analysis, Delineation*

***R**eceived 03 May, 2022; **R**evised 14 May, 2022; **A**ccepted 16 May, 2022 © The author(s) 2022.*
P**ublished with open access at **www.questjournals.org

I. INTRODUCTION

The officer basin is one amongst several intracratonic, Neoproterozoic to early Palaeozoic, basins with similar characteristics, trending E-W in existence within the central portion of Australia (*Figure 1)* characterised by their large negative Bouguer gravity anomalies with amplitude in excess of 150*mGal* [1]. It is the largest of the present day intracratonic basins with an estimated area of about $4 \times 10^5\ km^2$ [2, 3]. It is bounded by the Eromanga Basin in the East; the Canning Basin and Musgrave Block in the north; the Eucla Basin in the South; and mainly by the Yilgarn block and Bangemall Basin in the West [4].

Central Australia, where the Officer Basin is located, has gone through series of geological evolution characterised by a long history of metamorphism, plutonism and the reworking of the crust[1]. In her work, *Lindsay [5]* explained the early evolution of the Basin based on the existence of a Proterozoic super continent and the timing of its break-up as postulated by Bond *et al* [6].

The Officer Basin forms an elongated E-W trending trough, distinctly asymmetric in N-S profile with its northern margin characterised by a sharp, thrust fault against the Musgrave Block (*Figure 1*), over thrust to the south [1]. The Grawler Craton, at the south-eastern boundary (*Figure 1*), delimits the Officer Basin at this boundary with a number of deep, intervening sub-basins running parallel to the margin. The Basin broadens out to the south forming a shallow platform gradually rising from the northern axis.

With sedimentary succession classified into six megasequences characterised by major tectonically and erosionally enhanced sequence boundaries, with distinctive sequence pattern, the sediments in the Officer Basin is suggested to have been deposited in response to an episodic subsidence induced by a major extrinsic tectonic event [2].

Data obtained from deep reflection seismic profiles, teleseismic travel-times studies and seismic refraction have been very useful in providing information about the deep crustal structure beneath the central Australian Basins and the intervening Basement blocks [1]. According to Lindsay *et al* [2], the crust on which the central Officer Basin rest is approximately 42km thick as deduced form deep reflection seismic profile, with the sediments at the eastern Officer Basin estimated at being 5-6Km.

Also, seismic reflection profile to the area north of the Officer Basin shows the displacement of the Moho that has been enhanced by thick-skinned deformation of the crust which is suggested to be primarily

responsible for the observed Bouguer gravity anomaly, where the crust/mantle boundary have been offset by due to thick-skinned thrusting [7].

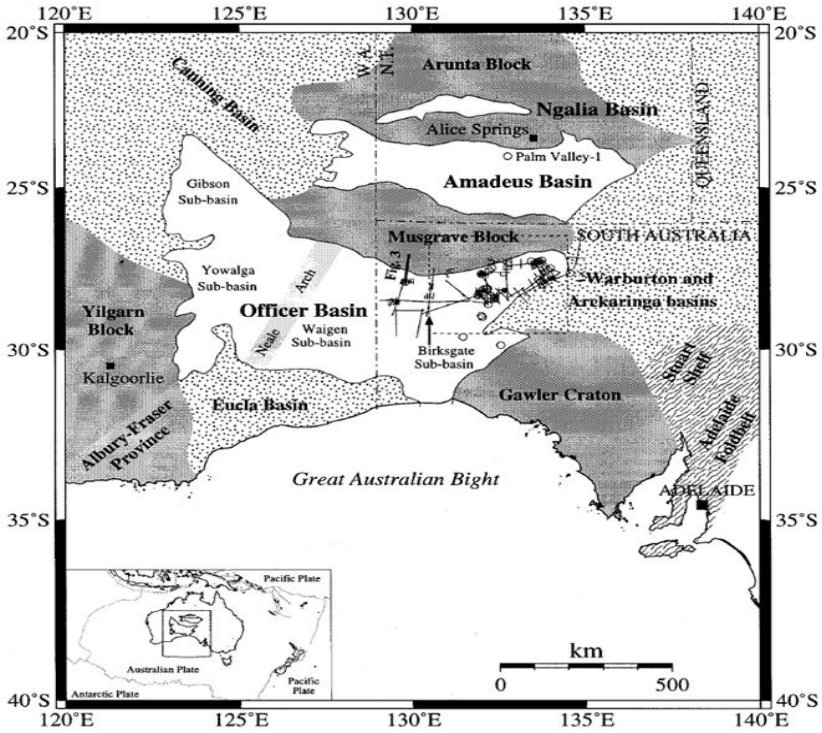

Figure 1: Location of the officer Basin [1]

Bouguer anomaly is the gravity anomaly after necessary corrections have been carried out due to other sources different from the source under investigation [8]. In other words, it is the difference between the expected gravity value at a given location (with an additional function of the effect of latitude, longitude, altitude and the rotation of the earth) and its actual value. Since magnetic field is a vector quantity, i.e. it is direction dependent, the total magnetic intensity (TMI) is the estimated magnetic anomaly due to the presence of a magnetic body within the earth's magnetic field as a result of the anomalies in all possible direction (easterly intensity, northerly intensity and Vertical intensity). TMI is therefore the most practical way to measure magnetic anomalies [9].

Compared to gravity anomalies, magnetic anomalies due to most geological structures have an added complexity as a result of the earth's field [10]. Apart from the physical properties of the source, without the consideration of remnant magnetization, the magnetic anomaly also depends on the position and direction of the geomagnetic field [11]. Therefore, reduction to pole (RTP) is a standard processing step for magnetic data, transforming an anomaly due to an arbitrary source into an anomaly due to the same source if it were magnetised by induction only and located at the poles, thereby centering the anomaly highs over the source of the anomaly. Furthermore, most of the transformative derivatives necessary for the interpretation of magnetic data are most effective when done on a data that has been reduced to the pole [12]. On a flip side, the process of reducing magnetic data to pole is trivial if there is a significant presence of remanence magnetization [13].

There is a general relationship between density and the susceptibility of geologic bodies such that high density geologic structures are often magnetically susceptible [14]. If this relationship is actually present, then the magnetic grid can be transformed to a pseudo-gravity grid, i.e. the gravity anomaly that would have been observed if the density and susceptibility of the causative geologic structure is the same [15]. Therefore, comparing gravity maps to pseudo-gravity map will better help to define the local geology as the coincidence of anomalies is probable due to the same geologic structure [16]. It is a very useful tool in the interpretation of magnetic data as it can be used in place of the reduced to pole magnetic grid in the presence of significance remanence magnetisation.

Horizontal derivative is a very useful in delineating contacts, especially in magnetic data [17]. However, until the magnetic data is reduced to pole, this derivative is not very useful as it is severely affected by inclination and hence will be inaccurate in indicating the true location of a contact [18]. Additionally it is not very useful on grid data as it duplicates features since it is very directional and therefore can't be depended upon

for mapping [18]. The directional horizontal derivative is easily calculated in the space domain as it doesn't require information on how the field diverges and decreases with height.

The total horizontal derivative proffers solutions to the problems introduced by the directional horizontal derivative [19]. It is more accurate in mapping edges compared to the directional horizontal derivative as it measures the full horizontal gradient. It is more effective in enhancing gravity data as its mapping as its maxima lies sufficiently close to the boundary causing the anomaly. On magnetic anomalies however, as defined by the total magnetic intensity, the data needs to be reduced to pole or converted to pseudo-gravity for the total horizontal derivative to be quite effective [20].

The vertical derivative is a very useful tool in resolving gravity and magnetic anomalies over individual structures especially because, as related to magnetic anomalies, it suppresses the regional content of the data [21], hence very useful in locating structures by defining the extent of the geological bodies. However the first vertical derivative is mostly estimated in the frequency domain and not in the space domain as it requires information on the divergence and decrease of the field with height for a better estimation, it is therefore calculated using the fast Fourier transform [22]. The second vertical derivative has the property assuming a zero value over contacts, hence qualitative interpretation based on the second vertical derivative is very limited to the edge locations by mapping the zero contours. However, because it is a second order derivative, it magnifies noise within the data set. This derivative is often estimated using the 1D fast Fourier transform [22].

The analytical signal method is also known as the total gradient method which is a quite useful interpretational tool for profile and grid data of gravity and magnetic anomalies. It is simply a Pythagorean sum of horizontal and vertical derivatives resulting in a positive anomaly with peaks directly over the top of contacts, with local maxima over the edges of magnetic structure [23]. However, it somewhat has a lower resolution and noisier than horizontal derivatives and because it involves estimations made from the vertical derivative, it is often estimated using the 1D Fast Fourier transform [22]. It is very important to note that the amplitudes of the total horizontal derivative, the vertical derivative and the analytical signal is dependent on magnetisation and hence cannot map all anomalies [17].

In the analysis of potential field, the vertical and horizontal derivatives of gravity and reduced to pole magnetic data are limited, even though they are sometimes efficient in mapping the lateral extent of the geological bodies and their edges, since the gravity and magnetic anomalies are largely dependent on the density and susceptibility contrast present [24]. Therefore, the larger the contrast, the larger the anomaly and vice versa. This factor is also transferred unto the horizontal derivative, vertical derivative, and analytical signal such that it may be quite difficult to map smaller anomalies in the presence of large amplitude anomalies. The tilt derivative however is independent of magnetisation, and therefore is a better tool in mapping these anomalies irrespective of their amplitudes. It is the physical property of a magnetic source that can be estimated from a magnetic data that is very useful in defining the shape, location of its edges, depth to top edges, dip and rock susceptibility contrast [18]. Mathematically, it is the arc-tan of the ratio of the horizontal derivative to the vertical derivative.

One very effective property used for interpreting magnetic data is the local wavenumber of the magnetic anomalies. It is often preferred as an alternative to analytical signal amplitude because even though they are both independent of the ambient magnetic field and the direction of dip, the local wavenumber is better resolved with its maxima inversely proportional to the depth of the contact [25].

The ridge grid method is an automatic lineament mapping algorithm. However, it is most efficient when the data have been processed so that the edge of the body lies at the peak of the anomaly. This can be achieved by different methods, obvious choices including horizontal derivative of the RTP or pseudo-gravity [26], Analytical signal [27] and the local wave number.

The report is aimed at presenting a regional scale interpretation, which will be focused mainly on mapping the shape of the basin and the basement depth, of the poorly explored Officer basin in offshore Australia with an objective of mapping and identifying geological features within the basin based on grids of gravity and magnetic data.

II. METHODOLOGY

The entire Interpretation will be done on grids of gravity and magnetic data which are subsets of regional grids for the entire Australia, mapped with a standard geoscience Lambert conic projection, focused around 122-134^{o}E and 31-22^{O}S. Additionally, the magnetic data is part of a high-resolution aeromagnetic survey where the total magnetic intensity, with estimated magnetic inclination and declination in the area at approximately -59.5^{O} and 3.5^{O} respectively.

To further aid interpretation of the geological structure and basement depth within the Officer Basin, certain enhancement tools (which have been summarised in appendix A1) were used. Two software were used to aid interpretation from the grids; GETGRID on which the enhancement tools were applied and ARCGIS on which the interpretation on the grids produced by the enhancement tools was made.

2.1 Structural Mapping

Beginning by mapping the maximum and minimum anomalies on the Bouguer anomaly and the reduced to pole grid of the total magnetic intensity and then comparing it to lows and highs on the pseudo gravity to map structural lows and highs.

The Analytical signal of the reduced to pole TMI was then used to map the edge of the Officer Basin as the local maxima of the anomaly was directly over the edge.

2.2 Lineament Analysis

For the delineation of basement lineaments, the total horizontal derivative of the magnetic anomaly was the primary source from which the interpretation was based because apart from positioning the maxima of these anomalies over the edge of the source of the anomaly, it is also less noisy compared to the analytical signal, aided by a ridge grid of the total horizontal derivative. Amongst these contacts were faults whose direction of throw was defined relative to the position of the size of the anomaly along the mapped fault, with the fault throwing in the direction of low density and/or susceptibility.

To determine what type of faults that was mapped, the mapped faults from total horizontal derivative of the magnetic anomaly were overlain on the total horizontal derivative of the Bouguer anomaly and the position of the maxima relative to the position of the fault was compared, knowing that if the maxima is on the up thrown side of the fault it is reverse fault and if the maxima is on the down thrown side of the fault it a normal fault [28].

2.3 Delineation of Sub-Basins

Furthermore, Sub Basins within the Officer Basin was mapped. This was determined by comparing the minimum anomaly on the grid of the Bouguer anomaly to the grid of the Pseudo gravity obtained from the total magnetic intensity and mapping Sub Basins as matching structural lows on both anomalies, i.e. anomalies that are the lowest anomalies on the Bouguer anomaly and also low on the Pseudo Gravity.

2.4 Depth Estimation

Although there were different methods of depth estimation from magnetic and gravity data (e.g. the Tilt-depth method, Depth slicing, Local wave number), the depth to basin within the Interpreted Officer Basin was mapped using the Tilt-depth method as it was straight forward and less prone to errors compared to the Local wave number [29], which is actually a third-order derivative and therefore prone to noise, or the depth slice method, which estimates an average depth over particular region. The depth estimation through the tilt-depth method was made even more effective by conditioning the grid such that the grid only showed contours between -45^{o} and $+45^{o}$ such that half the length of the anomaly at any point is the depth at that point.

III. RESULTS/INTERPRETATION

3.1 Mapped Structures

3.1.1 Gravity Low and High (Bouguer Anomaly)

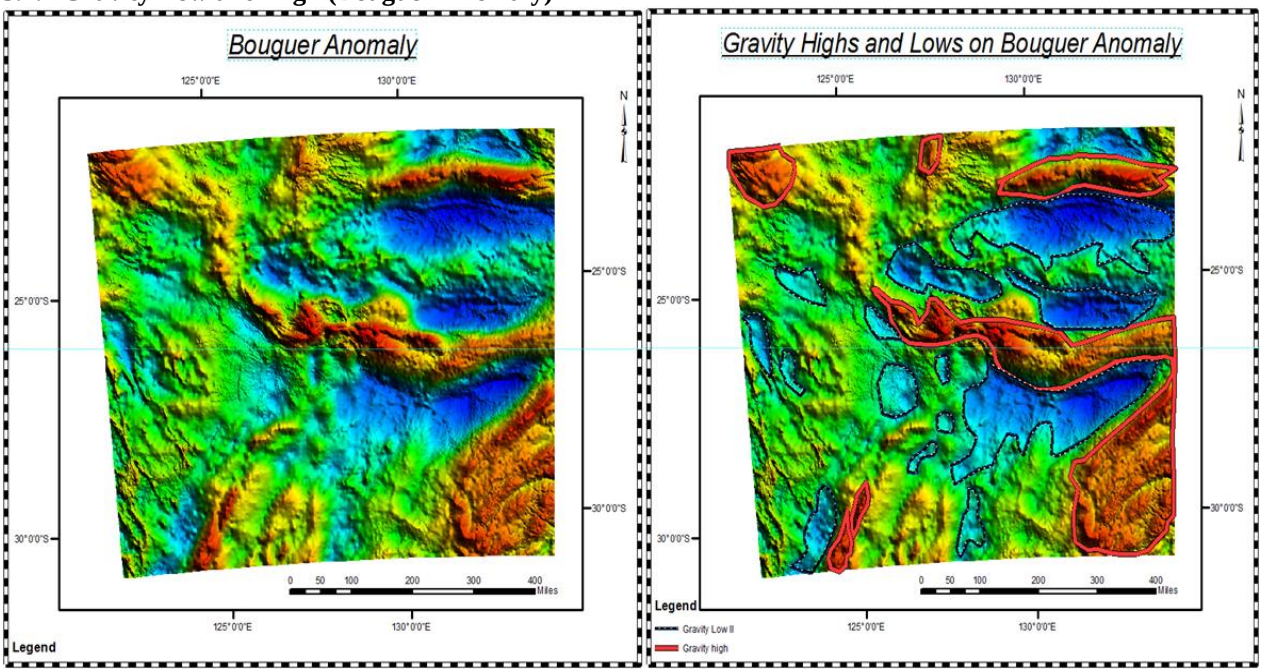

Figure 2: Mapped Highs and lows on the Bouguer Anomaly

On *Figure 2* are two grids showing the grid of Bouguer anomaly, on the image on the left and the same grid with the gravity lows (annotated with blue polygons) and the gravity highs (annotated with red polygons) on the image on the right indicative of the regions with lowest and highest density, in other words structural lows and highs, within the survey area.

3.1.2 Magnetic Low and High (RTP of the TMI)

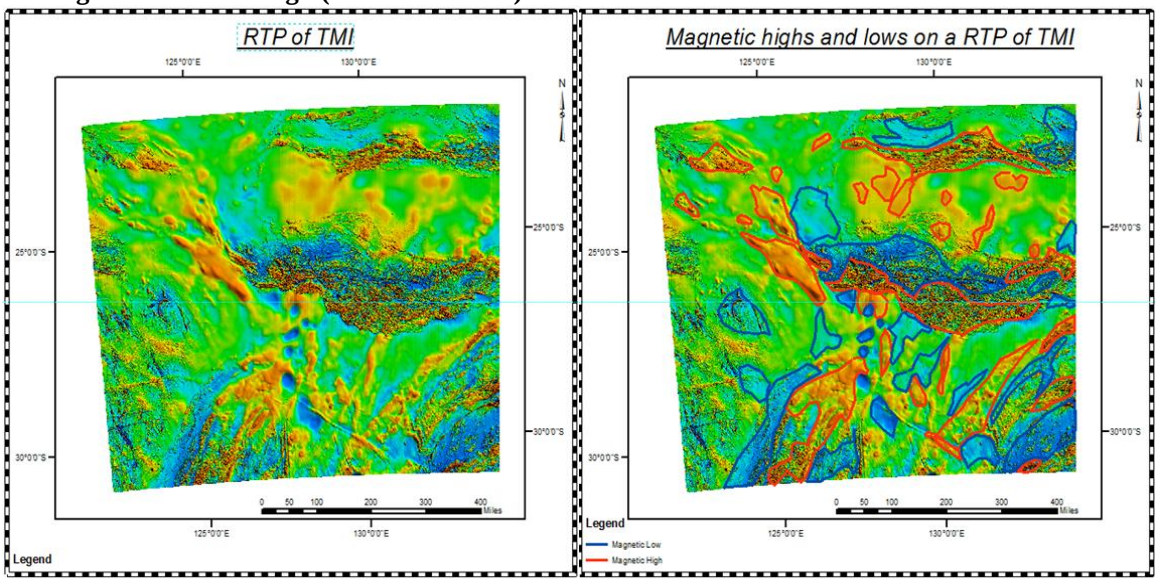

Figure 3: Mapped Highs and Lows on the magnetic anomaly

Similarly, as was done for the gravity anomalies, the highs and the lows have been identified on the magnetic anomaly, however on a grid of the magnetic anomaly that have been reduced to pole to correct the magnetic anomalies relative to the poles. The image on the left in *figure 3* is the total magnetic field that was measured while the image to the right is the reduced to pole grid on which the lows and highs have been mapped with blue and red annotations respectively, indicative of the minimum and maximum magnetic susceptibility within the survey area with the high frequency anomalies indicative of shallow structures and the low frequency anomalies indicative of deeper structure.

3.2 Analysed Lineaments

3.2.1 Edge of Basin

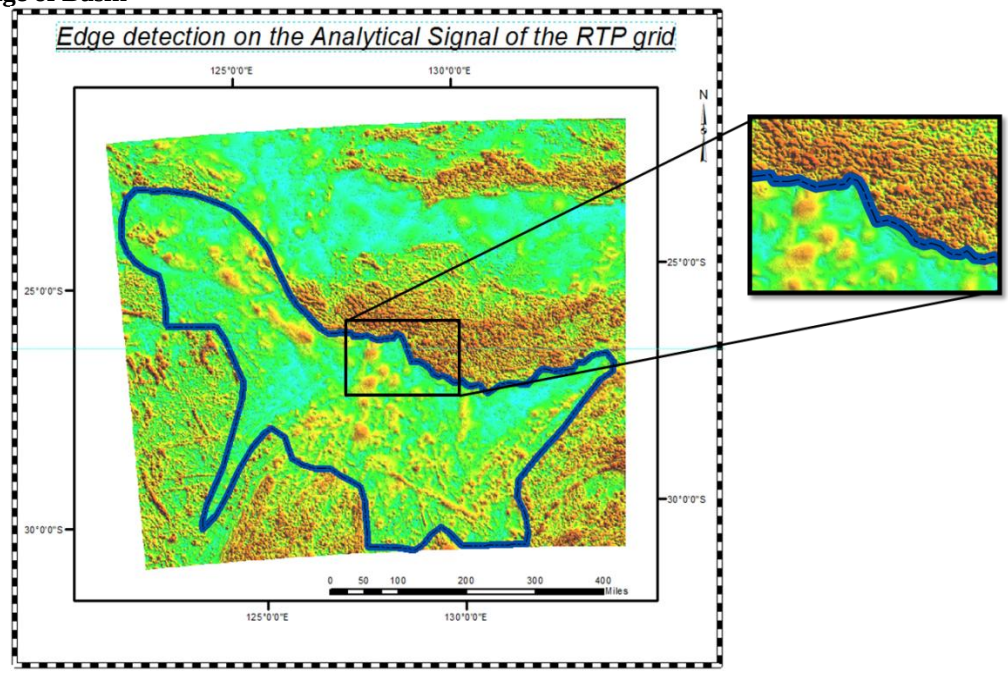

Figure 4: Mapped Edge of the Officer Basin

With the aid of the analytical signal of the RTP grid, the edges of the basin were mapped on the grid as shown on *Figure 4*, trending NW-SE.

3.2.2 Linear & Non-linear Structures

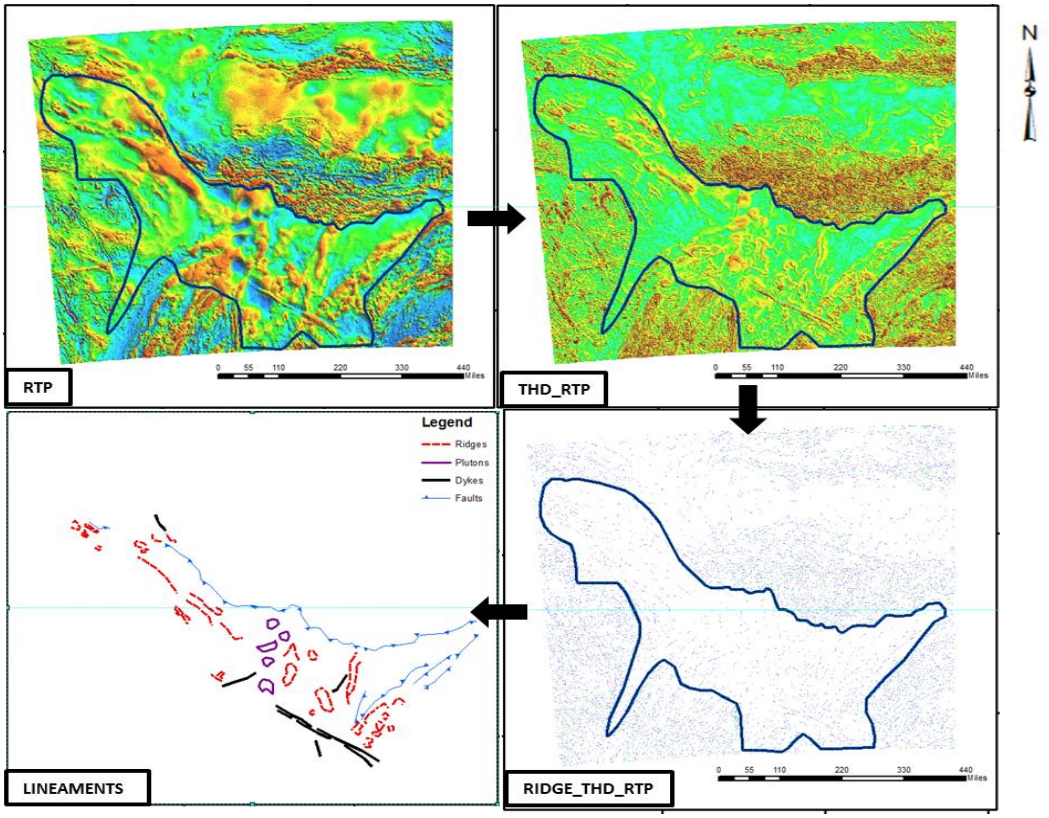

Figure 5: Mapped Lineaments within the officer Basin

For mapping basement lineaments, the ridge grid, which automatically maps contact, of the total horizontal derivative of the reduced to pole TMI was placed over it and used to map some lineaments, both linear and non-linear, within the Basin. The mapped lineaments include faults, Ridges, Dykes and Plutons. Most of the mapped faults were throwing into the Officer Basin indicated by the low magnetic anomaly, i.e. low susceptibility in the direction of throw. The major faults mapped are thrust faults.

3.3 Delineated Sub-Basins

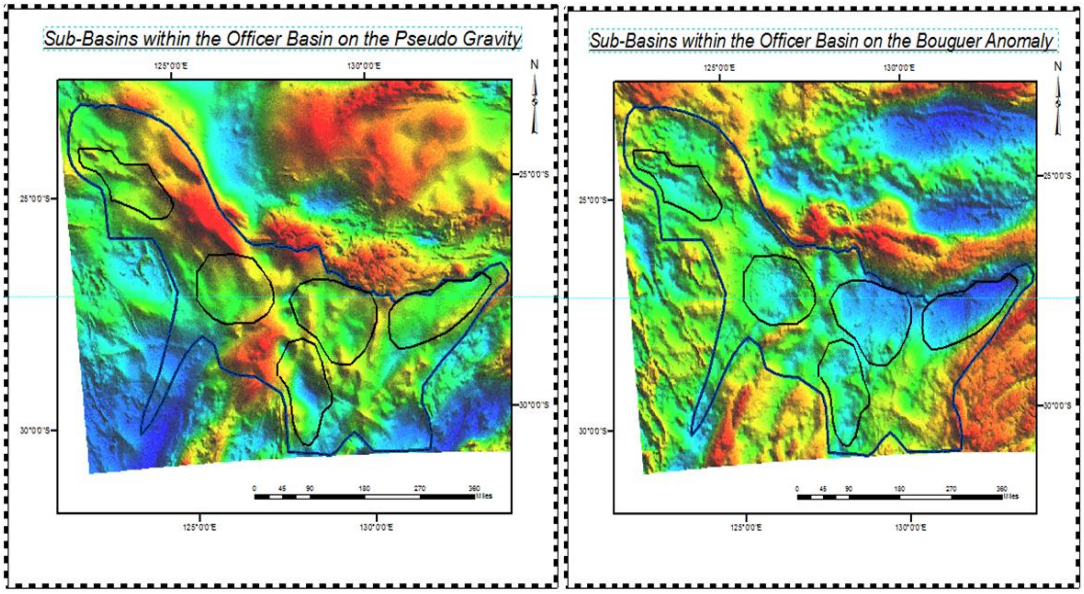

Figure 6: Sub-Basins within the Officer Basin

Within the Officer Basin, five (5) Sub-Basins were mapped by identifying structural lows on the Bouguer Anomaly that matched structural lows on the pseudo-gravity. However, there are certain lows on the Bouguer anomaly which can be seen as highs on the pseudo gravity, indicating a region of high susceptibility and low-density contrast relative to the surrounding rock rather than a structural low These Sub-Basins are shown in *Figure 6.*

3.4 Estimated Depths

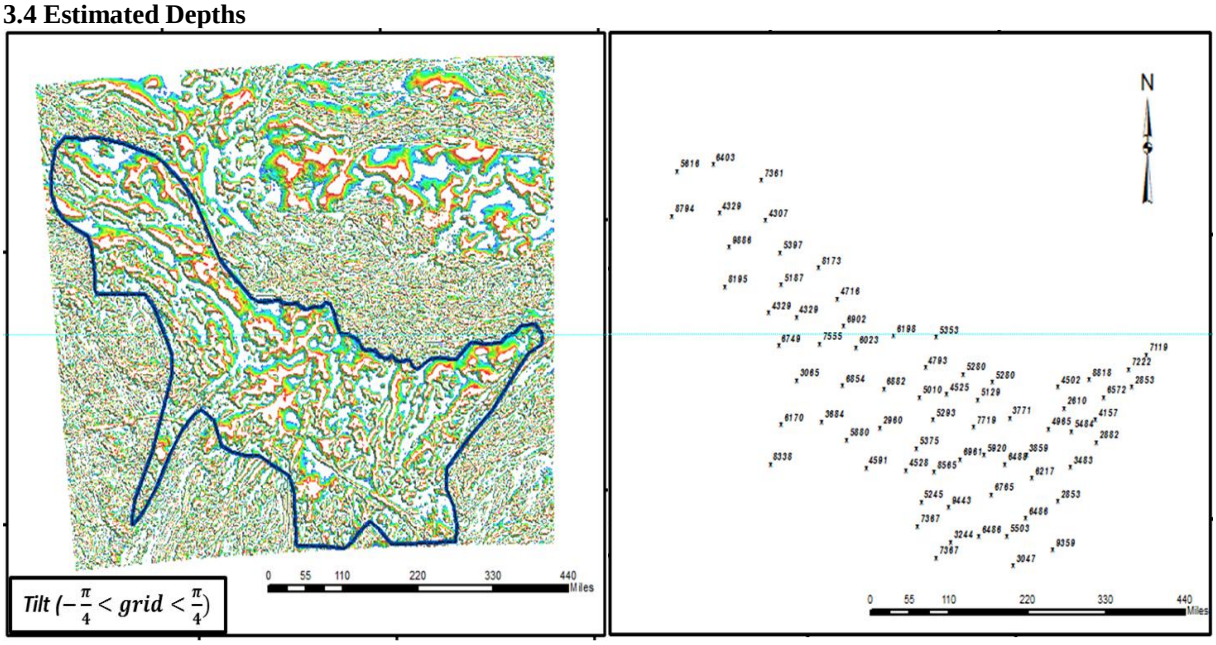

Figure 7: Mapped depths to basement within the Officer Basin

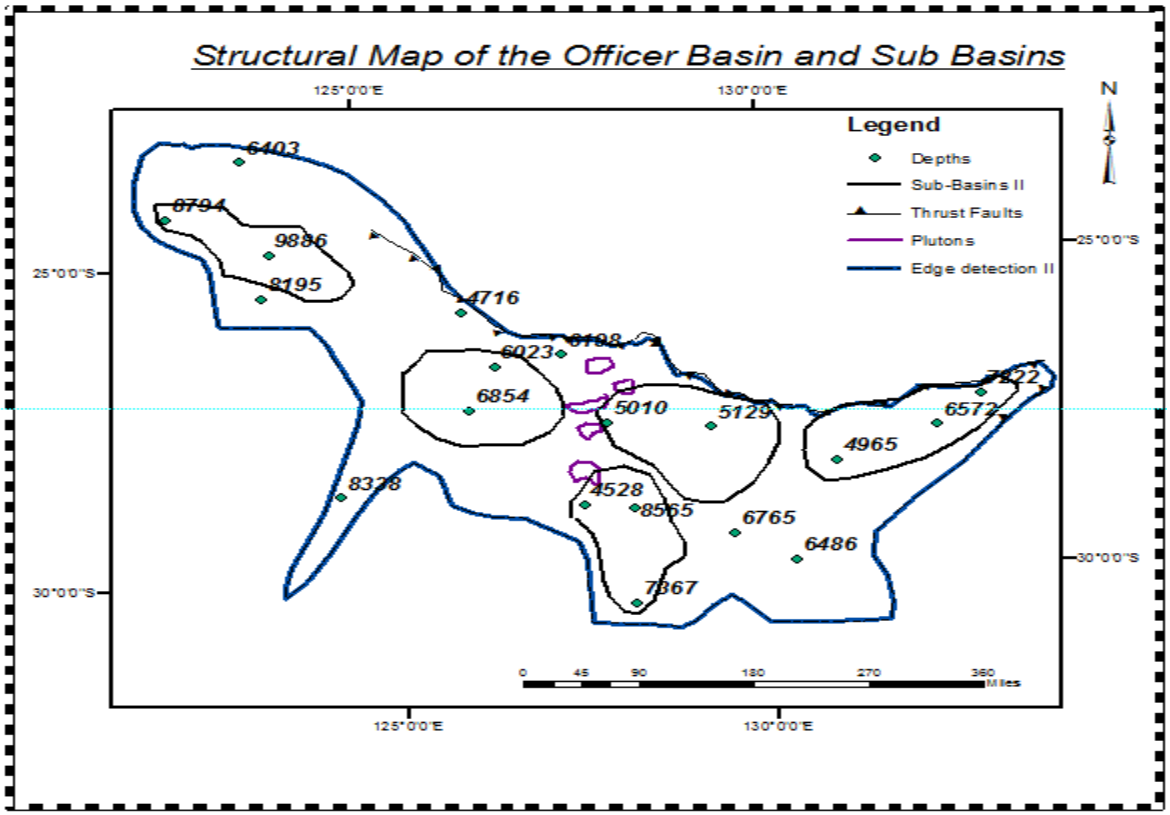

Figure 8: Structural map of the Officer Basin showing major structures and key features

The estimated depths showed that the deepest part of the Officer Basin is located at about 9.8km below the subsurface while its shallowest part was about 4.5km below the subsurface.

IV. DISCUSSIONS

So far, the edges and some structures within the Officer Basin have been mapped within the limits of the data provided and the methods employed in the interpretation. Therefore, the accuracy of these interpretations is subject to the limitation of the methods employed during interpretation.

One major source of error is in the estimation of the depths within the officer Basin. These estimated depths are really subjective, pending further interpretation from other geophysical methods. The tilt depth method that have been used in estimating depths in this report is prone to producing shallow depth estimates in areas where the contacts are not vertical [30].

Also, in comparing the edge and shape of the Basin mapped to the shape of the Officer Basin in *Figure 1*, there are evident differences in the shape of the Basin. This may be due to errors arising from the fact that analytical signal of the reduced-to-pole grid of the total magnetic intensity that was used in delineating the edges of the basin has poorly resolved shallow structures and therefore the edge of the Basin delineated may be the edge of the Basin deep into the formation and not the edge at the surface.

These sources of errors can be best constrained by the availability of data from further exploration of the Officer Basin.

V. CONCLUSION

Aimed at presenting a regional scale interpretation, focused mainly on mapping the shape of the basin and the basement depth of the Officer basin in offshore Australia, mapping and identification of geological features within the basin, based on grids of gravity and magnetic data, have been carried out in this research.

- Within the Officer Basin, five Sub-Basins have been mapped with the largest of these Sub-Basins to the far east of the Basin with the deepest part of the Basin lying West of the Officer Basin within one of the Sub-Basin at an estimated depth of 9.8km.
- Among the lineaments mapped within the Basin is a large thrust fault at the Northern Edge of the Basin dipping SW, group of plutons all running along the centre of the Basin, along the Neale Arch, dykes and ridges.

ACKNOWLEDGEMENT

The authors would want to acknowledge The School of Earth and Environment of the University of Leeds, Leeds, United Kingdom, for providing the resources needed for this work.

REFERENCES

[1] Haddad, D., A. Watts, and J. Lindsay, *Evolution of the intracratonic Officer Basin, central Australia: implications from subsidence analysis and gravity modelling.* Basin Research, 2001. **13**(2): p. 217-238.
[2] Lindsay, J.F. and J.H. Leven, *Evolution of a Neoproterozoic to Palaeozoic intracratonic setting, Officer Basin, South Australia.* Basin Research, 1996. **8**(4): p. 403-424.
[3] Wade, B., M. Hand, and K. Barovich, *Nd Isotopic and Geochemical Constraints on Provenance of Sedimentary Rocks in the Eastern Officer Basin, Australia: Implications for the duration of the Intracratonic Petermann Orogeny.* Journal of the Geological Society, 2005. **162**(3): p. 513-530.
[4] Cawood, P.A. and R. Korsch, *Assembling Australia: Proterozoic building of a continent.* Precambrian Research, 2008. **166**(1-4): p. 1-35.
[5] Lindsay, J.F., *Sequence stratigraphy and depositional controls in Late Proterozoic-Early Cambrian sediments of Amadeus Basin, central Australia.* AAPG Bulletin, 1987. **71**(11): p. 1387-1403.
[6] Bond, G.C., P.A. Nickeson, and M.A. Kominz, *Breakup of a supercontinent between 625 Ma and 555 Ma: new evidence and implications for continental histories.* Earth and Planetary Science Letters, 1984. **70**(2): p. 325-345.
[7] Goleby, B.R., et al., *Geophysical evidence for'thick-skinned' crustal deformation in central Australia.* Nature, 1989. **337**(6205): p. 325-330.
[8] Balmino, G., et al., *Spherical Harmonic Modelling to ultra-high Degree of Bouguer and Isostatic Anomalies.* Journal of Geodesy, 2012. **86**(7): p. 499-520.
[9] Munschy, M. and S. Fleury, *Scalar, vector, tensor magnetic anomalies: Measurement or computation?* Geophysical Prospecting, 2011. **59**: p. 1035-1045.
[10] Luo, Y., D.J. XUE, and M. WANG, *Reduction to the pole at the geomagnetic equator.* Chinese Journal of Geophysics, 2010. **53**(6): p. 1082-1089.
[11] Lesur, V., et al., *Building the Second Version of the World Digital Magnetic Anomaly Map (WDMAM).* Earth Planets Space, 2016. **68**(1): p. 1-13.
[12] Fedi, M. and G. Florio, *Detection of Potential Fields Source Boundaries by Enhanced Horizontal Derivative Method.* Geophysical Prospecting, 2001. **49**(1): p. 40-58.
[13] Lelièvre, P.G. and D.W. Oldenburg, *A 3D Total Magnetization Inversion Applicable when Significant, Complicated Remanence is Present.* Geophysics, 2009. **74**(3): p. L21-L30.
[14] Borradaile, G.J. and M. Jackson, *Structural Geology, Petrofabrics And Magnetic Fabrics (AMS, AARM, AIRM).* Journal of Structural Geology, 2010. **32**(10): p. 1519-1551.
[15] Bott, M., R. Smith, and R. Stacey, *Estimation of the direction of magnetization of a body causing a magnetic anomaly using a pseudo-gravity transformation.* Geophysics, 1966. **31**(4): p. 803-811.
[16] Alamdar, K. and A. Ansari, Journal of the Earth and Space Physics, 2011. **37**(1).
[17] Pilkington, M. and P. Keating, *Contact Mapping from Gridded Magnetic Data? A Comparison of Techniques.* Exploration Geophysics, 2004. **35**(4): p. 306-311.

[18] Verduzco, B., et al., *New Insights into Magnetic Derivatives for Structural Mapping.* The leading edge, 2004. **23**(2): p. 116-119.
[19] Yuan, Y., D.-N. HUANG, and Q.-L. YU, *Using Enhanced Directional Total Horizontal Derivatives to Detect the Edges of Potential-field full Tensor Data.* Chinese Journal of Geophysics, 2015. **58**(7): p. 2556-2565.
[20] Florio, G., *Mapping the Depth to Basement by Iterative Rescaling of Gravity or Magnetic Data.* Journal of Geophysical Research: Solid Earth, 2018. **123**(10): p. 9101-9120.
[21] Paine, J., *A comparison of methods for approximating the vertical gradient of one-dimensional magnetic field data.* Geophysics, 1986. **51**(9): p. 1725-1735.
[22] Gunn, P., *Linear Transformations of Gravity and Magnetic FIELDS*.* Geophysical Prospecting, 1975. **23**(2): p. 300-312.
[23] Roest, W.R., J. Verhoef, and M. Pilkington, *Magnetic interpretation using the 3-D analytic signal.* Geophysics, 1992. **57**(1): p. 116-125.
[24] Oruç, B. and H.H. Selim, *Interpretation of Magnetic Data in The Sinop Area of Mid Black Sea, Turkey, Using Tilt Derivative, Euler Deconvolution, and Discrete Wavelet Transform.* Journal of Applied Geophysics, 2011. **74**(4): p. 194-204.
[25] Thurston, J.B. and R.S. Smith, *Automatic conversion of magnetic data to depth, dip, and susceptibility contrast using the SPI (TM) method.* Geophysics, 1997. **62**(3): p. 807-813.
[26] Cordell, L. and V. Grauch, *Mapping basement magnetization zones from aeromagnetic data in the.* The utility of regional gravity and magnetic anomaly maps, 1985: p. 181.
[27] Nabighian, M.N., *Toward a three-dimensional automatic interpretation of potential field data via generalized Hilbert transforms: Fundamental relations.* Geophysics, 1984. **49**(6): p. 780-786.
[28] Grauch, V., M.R. Hudson, and S.A. Minor, *Aeromagnetic expression of faults that offset basin fill, Albuquerque basin, New Mexico.* Geophysics, 2001. **66**(3): p. 707-720.
[29] Chen, Q., et al., *Applying the Tilt-depth and Tilt-Euler Techniques of Gravity Data to Decipher the Basement Depth in Sichuan Basin, China.* Acta Geophysica, 2021. **69**(6): p. 2173-2186.
[30] Salem, A., et al., *Sedimentary basins reconnaissance using the magnetic Tilt-Depth method.* Exploration Geophysics, 2010. **41**(3): p. 198-209.